

Crystal Structure and DNA Interaction of the Facial-Type *rac*-Tris[2-(aminomethyl)benzimidazole]cobalt(III) Complex

Jordi Gómez-Segura,^{*,†} María José Prieto,[‡] Mercè Font-Bardia,[§] Xavier Solans,[§] and Virtudes Moreno^{*,†}

Departament de Química Inorgànica, Universitat de Barcelona, Martí i Franquès 1–11, Departament de Microbiologia, Universitat de Barcelona, Diagonal 645, and Departament de Cristal·lografia, Minerologia i Dipòsits Minerals, Universitat de Barcelona, Martí i Franquès s/n, E-08028 Barcelona, Spain

Received July 13, 2006

rac-[Co(ambi)₃]Cl₃·3H₂O corresponds to a tris-chelate complex bearing 2-(aminomethyl)benzimidazole (ambi) ligands bound to the Co(III) ion in a facial-type fashion. The high metal *q/r* ratio and electronic delocalization between coordination heterocyclic functionalities can provide powerful tools to minimize DNA condensation, which arises from the neutralization of the negatively charged sugar phosphate backbone in the presence of multivalent [Co(ambi)₃]³⁺.

Small-molecule DNA-binding agents have attracted substantial research interest in the field of chemotherapy against cancer.¹ Thorough pharmacological studies have helped elucidate the mechanism by means of which small molecules interact with DNA via electrostatic force, groove binding, or intercalation. In particular, much attention has been focused on the so-called metallointercalators. These correspond to transition-metal complexes bearing planar aromatic heterocyclic functionalities that intercalate into the DNA base stack.²

Interestingly, metal ions play an important role in biological processes and the mechanism of metal-targeted organic drugs against cancer.³ To modulate the binding of minor-groove targeted oligomers bearing repetitive benzimidazole units, Co(III) octahedral complexes of 2-(aminomethyl)benzimidazole (**1**, ambi) have been proposed as functional models for prospective hypoxia-selective cytotoxins.⁴ On the other hand, the shape, size, and symmetry of octahedral transition-metal complexes can be exploited to develop

noncovalent binders that target specific DNA sites. On this basis, incipient studies were aimed at probing the DNA interaction with approximately spherical Ru complexes of polypyridyl ligands, metallointercalators, or combinations thereof.⁵ However, although chiral tris-chelate complexes of octahedral parentage offer the potential for enantioselective recognition of DNA, a mixture of binding modes to DNA can occur simultaneously such as electrostatic interaction, hydrophobic binding, and partial intercalation.⁶

Herein, we report the crystal structure and DNA interaction of the tris-chelate Co(III) complex *fac*-[Co(ambi)₃]Cl₃·3H₂O (**2**). The facial shape, symmetry, and ring functionalities of complex **2** can be overall exploited to counteract DNA condensation uniquely arising from electrostatic force in the presence of multivalent [Co(ambi)₃]³⁺.

Racemic complex **2** crystallizes in the triclinic space group *P* $\bar{1}$. The unit cell contains four symmetrical molecules due to a crystallographic inversion center (Figure 1). The assembly of molecules **2** in the crystal packing is afforded by the overall weak C–H··· π interactions (2.802–2.893 Å) through which ligands **1** lie quasi-perpendicular. Besides, the chloride ions and waters of solvation are involved in a complex H-bonded network with the N–H groups of peripheral ligands **1** (N–H···O = 2.726–2.890 Å; N–H···Cl = 3.089–3.288 Å). Interactions are accomplished with H-bonded water molecules (2.685–3.038 Å) and with chlorides (O–H···Cl = 3.110–3.223 Å). The molecular structure of **2** corresponds to a distorted octahedral geometry

* To whom correspondence should be addressed. E-mail: virtudes.moreno@qi.ub.es.

[†] Departament de Química Inorgànica.

[‡] Departament de Microbiologia.

[§] Departament de Cristal·lografia.

(1) Feigon, J.; Denny, W. A.; Leupin, W.; Kearns, D. R. *J. Med. Chem.* **1984**, *27*, 450.

(2) (a) Lerman, L. S. *J. Mol. Biol.* **1961**, *3*, 18. (b) Jennette, K. W.; Lippard, S. J.; Vassiliades, G. A.; Bauer, W. R. *Proc. Natl. Acad. Sci. U.S.A.* **1974**, *71*, 3839.

(3) Guo, Z.; Sadler, P. J. *Angew. Chem., Int. Ed.* **1999**, *38*, 1512.

(4) (a) Ware, D. C.; Wilson, W. R.; Denny, W. A.; Rickard, C. E. *F. J. Chem. Soc., Chem. Commun.* **1991**, 1171. (b) Gable, R. W.; Hartshorn, R. M.; McFadyen, W. D.; Nunno, L. *Aust. J. Chem.* **1996**, *49*, 625. (c) Cardwell, T. J.; Edwards, A. J.; Hartshorn, R. M.; Holmes, R. J.; McFadyen, W. D. *Aust. J. Chem.* **1997**, *50*, 1009.

(5) (a) Erkkila, K. E.; Odom, D. T.; Baton, J. K. *Chem. Rev.* **1999**, *99*, 2777. (b) Coggan, D. Z.; Haworth, I. S.; Bates, P. J.; Robinson, A.; Rodger, A. *Inorg. Chem.* **1999**, *38*, 4486. (c) Onfelt, B.; Lincoln, P.; Norden, B. *J. Am. Chem. Soc.* **1999**, *121*, 10846.

(6) (a) Satyanarayana, S.; Dabrowiad, J. C.; Cjaores, J. B. *Biochemistry* **1992**, *31*, 9319. (b) Satyanarayana, S.; Dabrowiad, J. C.; Cjaores, J. B. *Biochemistry* **1993**, *32*, 2573. (c) Eriksson, M.; Leijon, M.; Hiort, C.; Norden, B.; Graslund, A. *Biochemistry* **1994**, *33*, 5031.

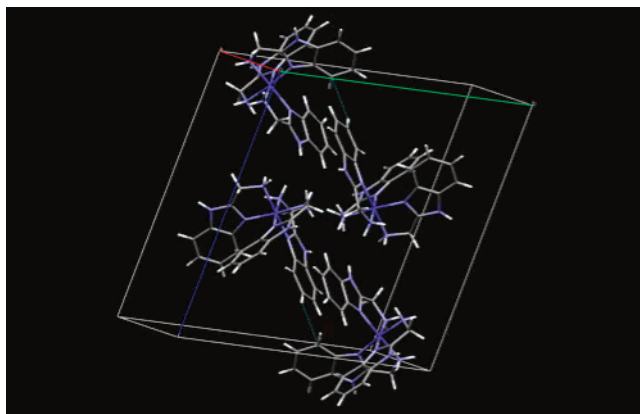


Figure 1. Crystal packing of complex **2** showing short contacts by weak C–H... π interactions (2.851 Å) between the two couples of Δ and Λ isomers in the unit cell.

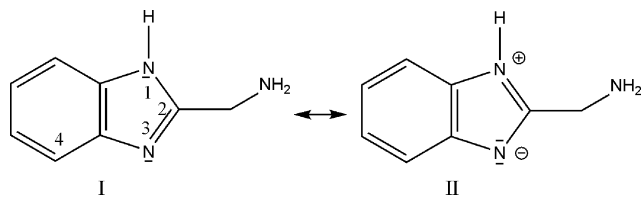


Figure 2. Resonance form representation of ligand **1**.

with a distribution of bond lengths and angles around the Co(III), as was so far reported for other similar structures.⁴ The three bidentate ligands **1** bind (chelate) to the Co(III) ion through the imidazole and amine N atoms, thereby forming five-membered rings. On this basis, the coordination geometry in a facial-type fashion makes the aromatic H4 atoms point directly toward the benzene ring of each adjacent ligand **1** (intramolecular C–H... π interactions ranging from 2.544 to 3.041 Å).

The covalent-bound Co(III) at position N(3) induces electronic reorganization through the heterocyclic ring functionalities of **1** (Figure 2).⁷ Taking advantage of the high metal q/r ratio and resonance form II, the release of protons at position N(1) can be attained in an aqueous solution influenced by ionic strength effects.⁸ To investigate the dissociation of the N–H bond imino proton in terms of the metal-withdrawing capability, mass conductivity measurements were directly monitored at room temperature as preliminary experiments. No matter what solvents were used to distinctly influence the dissociation constant, a drastic lowering of conductivity was unequivocally observed (Table 1). A plausible explanation for why a 1:1 electrolyte was measured could arise from the in situ formed 2-(aminomethyl)benzimidazolide ions $C_8H_8N_3^-$ (ambi') bound to the metal. Upon N–H bond dissociation, transient $[Co(ambi)_3]^{3+}$ is likely to afford monovalent cationic $[Co(ambi)_2(ambi)]^+$ in solution, hereinafter referred to as complex **4**. On the basis of univalent cations, **4** is hence expected to function as an efficient agent for probing the inhibition of DNA condensation.⁹

(7) (a) Harkins, T. R.; Walter, J. L.; Harris, O. E.; Freiser, H. *J. Am. Chem. Soc.* **1956**, *78*, 260. (b) Lane, T. J.; Nakagawa, I.; Walter, J. L.; Kandathil, A. *J. Inorg. Chem.* **1962**, *1*, 267.

(8) Lane, T. J.; Quinlan, K. P. *J. Am. Chem. Soc.* **1960**, *82*, 2994.

Table 1. Conductivity Measurements of Complex **2** in a 10^{-3} M Solution

solvent	Λ_M (cm ² /mol· Ω)	type of electrolyte ^a	
		1:1	1:3
DMF	73.80	65–90	200–240
MeOH	88.78	80–115	290–350

^a Range of conductivity for the most common metal complexes.¹⁰

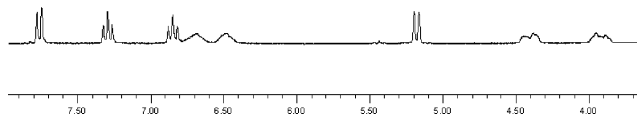


Figure 3. ¹H NMR spectrum of **2** in DMSO-*d*₆.

The ¹H NMR spectra of **2** were recorded at 25 °C in DMSO-*d*₆ (Figure 3) and H₂O/D₂O^{4b} to assign potentially informative resonances. The amino resonances exhibit a broad doublet centered at 6.68 and 6.48 ppm exclusively in DMSO-*d*₆ as the solvent. In regards to the molecular structure, this is consistent with two diastereotopic protons that are distinctly influenced by the field of an adjacent ligand **1**. By contrast, the imino resonances, presumably appearing downfield, were not evident from the ¹H NMR spectrum of **2**, which accounts for the enhanced lability. To confirm the ¹H NMR chemical shift associated with the imino resonances, an initial suspension of **1**·2HCl in EtOH was fully dissolved at 50 °C and subsequently added to HgCl₂ (1:1) in EtOH, yielding the diprotonated-ambi Hg(II) complex $[HgCl_4]-(H_2ambi)$ (**3**). The control ¹H NMR spectrum of **3** in DMSO-*d*₆ showed a broad signal centered at 8.65 ppm absent in H₂O/D₂O, which was unambiguously assigned, on the basis of its multiplicity, to the resonance of the three exchangeable protons bound at positions N(1) and N(3) (see the Supporting Information).

Atomic force microscopy (AFM) imaging provides direct evidence of DNA–drug interactions at the molecular level.¹¹ Upon interaction of **4** with 550-bp (base pair) linear DNA, approximately 50% of the fragments remained unaltered (Figure 4a), which may tentatively suggest different binding affinities of the Δ and Λ isomers for DNA. Chiral recognition of DNA via electrostatic interactions requires multivalent complexes to bind selectively at the sites of greatest negative electrostatic potential.¹² By contrast, the circular dichroism spectra of linear DNA and the racemic mixture of **2** in solution did not provide clear evidence of structural perturbations. In a separate experiment, circular plasmid pBR322 DNA was subjected to electrophoresis on an agarose gel. DNA migration into the gel exhibited neither reduced mobility nor strand scission after incubation with **4**. Therefore, the ease of dissociation involving the presence of some ramified aggregates imaged by AFM was attributed, in the

(9) Reimer, D. L.; Zhang, Y. P.; Kong, S.; Wheeler, J. J.; Graham, R. W.; Bally, M. B. *Biochemistry* **1995**, *34*, 12877.

(10) Geary, W. J. *Coord. Chem. Rev.* **1971**, *81*.

(11) (a) Coury, J. E.; McFail-Isom, L.; Williams, L. D.; Bottomley, L. A. *Proc. Natl. Acad. Sci. U.S.A.* **1996**, *93*, 12283. (b) Coury, J. E.; Anderson, J. R.; McFail-Isom, L.; Williams, L. D.; Bottomley, L. A. *J. Am. Chem. Soc.* **1997**, *119*, 3792.

(12) Fry, J. V.; Collins, J. G. *Inorg. Chem.* **1997**, *36*, 2919 and references cited therein.

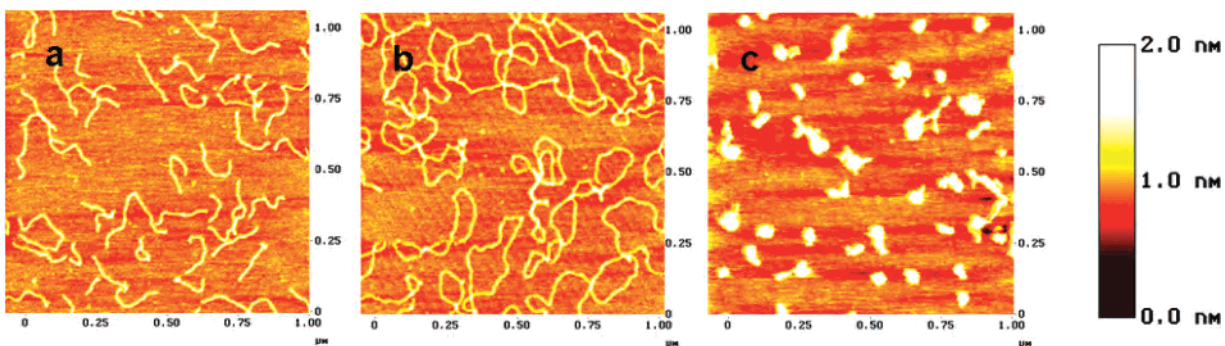


Figure 4. AFM images of DNA incubated at 37 °C for 5 h with complex **4** at ratio 1:1: (a) 550-bp linear DNA; (b) circular plasmid pBR322 DNA; (c) circular plasmid pBR322 DNA imaged at 7 days postincubation.

absence of conformational transition of the plasmid DNA,¹³ to noncovalent DNA-mediated interactions, i.e., the contribution of minimized electrostatic force and/or hydrophobic weak C–H··· π interactions to condensation.

Counterion-induced DNA condensation is a well-known electrostatic phenomenon attributed to the neutralization (~90%) of the negatively charged phosphate backbones.¹⁴ The DNA bp to complex ratio used for the linear DNA fragments and multivalent [Co(ambi)₃]³⁺ (1:1) enables one to compensate for amply more than 90% of the negative charge for condensing. However, decreased ionic strength caused by transient **2** to afford unipositive **4** does not lead to condensation of the DNA structure when bound to the proximity of the negatively charged phosphate backbones. To complement the aforementioned studies, plasmid pBR322 DNA was incubated with **4** and characterized by AFM and electrophoresis experiments. First, a freshly prepared sample exhibited some side-by-side association of DNA segments by AFM (Figure 4b). Subsequently, the stock solution containing pBR322 DNA–drug complexes was left undisturbed in the dark at room temperature. Aliquots of the sample were daily imaged by AFM, revealing subtle incipient changes of the morphology at 3 days postincubation, whereupon DNA evolved, progressively coarsening into nontoroidal aggregates (Figure 4c) at 7 days postincubation owing to the eventual crystallization induced by trivalent **2**.¹⁴

Gel electrophoretic separations (Figure 5) manifested changes in the DNA mobility associated with form I within an applied electric field. At 2 weeks postincubation, a very small proportion of the slower-moving form I with respect to the supercoiled DNA control was observed (Figure 5). By contrast, the migration of form II into the gel indicated almost no significant change or further accumulation as when supercoils are relaxed by nicking. A plausible explanation

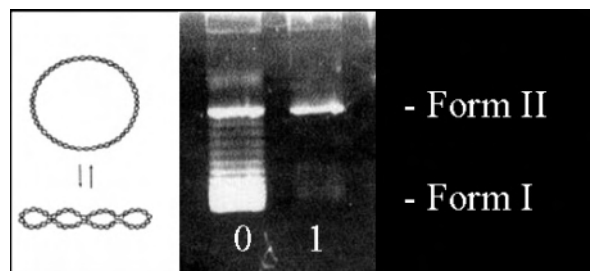


Figure 5. Supercoiled closed circular pBR322 DNA (form I) and open circular pBR322 DNA (form II): (a) DNA alone (lane 0); (b) DNA after incubation with **4**.

of this could be the screening caused by an excess of monovalent ions in TE buffer (50 mM NaCl, 10 mM tris(hydroxymethyl)aminomethane hydrochloride, 0.1 mM EDTA, pH 7.4) reducing the bridging effect of trivalent ions to condensation.¹⁵ Regardless, the observation of the open circular DNA control provides further evidence suggesting an uncondensed state.

In conclusion, complex **4** is prone to counteracting DNA condensation rather than accelerating it.¹⁶ The metal q/r ratio and ring functionalities can be exploited to modulate the binding affinities of multivalent complexes, thereby offering potential applications in chemotherapy against cancer and careful control of the DNA condensation reaction in gene therapy.

Acknowledgment. This work was supported by the Spanish Ministerio de Ciencia y Tecnología (Grant BQU-2002-0061).

Supporting Information Available: Experimental details and crystallographic data for **2** and **3**. This material is available free of charge via the Internet at <http://pubs.acs.org>.

IC061292T

(13) Arscott, P. G.; Ma, C.; Wenner, J. R.; Bloomfield, V. A. *Biopolymers* **1995**, *36*, 345.

(14) Bloomfield, V. A. *Curr. Opin. Struct. Biol.* **1996**, *6*, 334 and references cited therein.

(15) De la Cruz, M. O.; Belloni, L.; Delsanti, M.; Dalbiez, J. P.; Spalla, O.; Drifford, M. J. *Chem. Phys.* **1995**, *103*, 5781.

(16) Zheng, J.; Li, Z.; Wu, A.; Zhou, H.; Bai, H.; Song, Y. *Biochem. Biophys. Res. Commun.* **2002**, *299*, 910.